Fabrication of nGO/pGO-NanoCellulose Composite Membranes for Salinity Reduction in Domestic Water Treatment

Do Tam Nhu[1], Nguyen Phu Quy [1], Nguyen Huynh Quynh Anh[1], Dang Vu Bich Hanh[1], Nguyen Van Phuoc[2], Pham Thi Phuong Duyen[3,*]

[1]Faculty of Environment and Natural Resources, Ho Chi Minh City University of Technology, Vietnam National University Ho Chi Minh City (VNU-HCM)

[2]Ho Chi Minh City Union of Science and Technology Associations

[3]Biotechnology Center of Ho Chi Minh City (HCMBIOTECH)

Abstract

Saltwater intrusion in the Mekong Delta has become increasingly severe due to climate change and sea level rise, leading to a critical shortage of freshwater for domestic use in many coastal provinces of Vietnam. Conventional desalination technologies such as reverse osmosis (RO), electrodialysis (ED), multi-stage flash distillation (MSF), and multi-effect distillation (MED) are often associated with high operational costs, significant energy consumption, and limited applicability in rural and small-scale conditions. Therefore, the development of sustainable, low-cost, and environmentally friendly desalination materials is urgently needed. In this study, nanocellulose was successfully extracted from banana pseudostem waste through alkaline treatment, bleaching, and acid hydrolysis processes. Nitrogen/phosphorus-doped graphene oxide (n-pGO) was synthesized using a modified Hummers method. A green nanocomposite membrane based on nanocellulose and n-pGO was subsequently fabricated via a multi-layer coating approach on a nanocellulose substrate. In addition, a 10L pilot-scale filtration model was designed to evaluate the practical desalination performance of the developed membrane. The obtained nanocellulose/n-pGO membrane exhibited excellent desalination efficiency with salt rejection exceeding 97% and a stable permeation flux ranging from 160–180 $L \cdot m^{-2} \cdot bar^{-1}$ under atmospheric pressure conditions. The treated water satisfied most requirements of QCVN 01-1:2024/BYT for domestic water quality, including significant total dissolved solids (TDS) reduction, turbidity below 0.2 NTU, and complete removal of E.coli and Coliform bacteria. Furthermore, the membrane demonstrated enhanced antibacterial activity, strong antifouling performance with a flux recovery ratio (FRR) above 85% after multiple cycles. These findings indicate that the integration of banana-derived nanocellulose with doped graphene oxide offers a promising green nanocomposite membrane for low-cost and sustainable desalination applications, particularly for saline-affected regions in Vietnam.

Keywords: Nanocellulose, graphene oxide, nanofiltration membrane, banana stem, desalination.

1. Introduction

Currently, saltwater intrusion has emerged as one of the most critical environmental challenges in the Mekong Delta, Vietnam's key agricultural and economic region. Driven by the concurrent impacts of climate change, sea-level rise, prolonged droughts, and diminished upstream flows from the Mekong River, salinity intrusion has evolved into a highly complex phenomenon,

expanding in both geographical scope and intensity. During recent dry seasons, the 4‰ salinity boundary penetrated 25–90 km inland depending on local hydrological conditions and seasonal timing, directly disrupting domestic water supplies and agricultural production across provinces such as Ben Tre, Long An, Tien Giang, Soc Trăng, Kien Giang, and Ca Mau [1, 2]. Recent reports corroborate that the 2025–2026 dry season continues to induce acute domestic water shortages for hundreds of thousands of households in this region. Beyond degrading freshwater resources for daily life, salinity intrusion inflicts severe losses on agricultural productivity, aquaculture, and overall food security, particularly across rural and coastal communities [3-5].

To mitigate this crisis, various desalination technologies have been investigated and deployed, including reverse osmosis (RO), nanofiltration (NF), electrodialysis (ED), multi-effect distillation (MED), and multi-stage flash (MSF). Nevertheless, most existing technologies suffer from significant drawbacks, such as high capital and operational costs, heavy energy consumption, the requirement for high-pressure systems, and a high susceptibility to membrane fouling or scaling during long-term operation [6, 7]. Specifically, RO technology - despite its widespread application - typically requires elevated operating pressures between 55 and 80 bar for seawater treatment, which incurs substantial energy costs [8]. Furthermore, conventional desalination infrastructure is generally tailored for industrial scales rather than small-scale or household applications in rural areas, where economic resources and technical infrastructure are inherently constrained. Consequently, there is an urgent need to develop novel membrane materials characterized by high efficiency, low cost, low-pressure operability, and environmental friendliness.

From early exploratory research, graphene oxide (GO) membranes have attracted significant attention due to their unique two-dimensional structure and inherent nanochannels, which facilitate rapid water transport and effective ion selectivity. The interlayer spacing of GO typically ranges from 0.83 to 1.05 nm; this feature, coupled with abundant oxygen-containing functional groups such as hydroxyl, epoxy, and carboxyl groups, enhances hydrophilicity and accelerates water transport through the membrane matrix [9-11]. Studies from the 2018–2019 period demonstrated that GO holds immense potential for NF and RO systems, offering high salt and pollutant rejection under lower operating pressures than conventional polymeric membranes [12]. A prominent example includes Valencia et al. (2019), who developed layered GO membranes with robust filtration performance by creating structured nanochannels for water transport [13]. However, early investigations also revealed that pristine GO membranes suffer from severe swelling and restacking when exposed to saline environments or high-ionic-strength solutions. This structural expansion and re-layering of GO nanosheets alters the interlayer spacing, thereby compromising ion selectivity, mechanical stability, and membrane lifespan during continuous operation [10, 14].

Subsequent studies during 2020–2023 focused on enhancing the structural stability of GO membranes by incorporating nanocellulose or other biomaterials to engineer more resilient composite systems. Nanocellulose variants, comprising cellulose nanocrystals (CNC), cellulose nanofibers (CNF), and bacterial nanocellulose (BNC) were utilized as reinforcing frameworks or

molecular spacers to regulate the interlayer distance between GO sheets via hydrogen bonding between the hydroxyl groups of cellulose and the oxygenated groups of GO [15]. For instance, H. Gao et al. (2021) employed CNCs as spacers within GO membranes, successfully constraining the interlayer spacing to approximately 0.65 nm and achieving over 99% rejection of multivalent ions along with superior antifouling properties [16]. Concurrently, A. Saud et al. (2022) comprehensively reviewed nanocellulose-based membranes for desalination, asserting that hybridizing nanocellulose with GO improves hydrophilicity, enhances mechanical strength, elevates water flux, and mitigates fouling compared to pristine GO membranes [17]. Nonetheless, composite membranes from this era still exhibited limitations, including flux decline over multiple filtration cycles, suboptimal long-term stability in highly saline media, and trade-off difficulties in simultaneously optimizing water flux and salt rejection [17, 18].

More recent research in the 2024–2026 period has shifted sharply toward the chemical modification of graphene oxide and the development of multifunctional nanocomposites to enhance both desalination performance and practical feasibility. Numerous studies have integrated heteroatom-doped graphene oxide, modified with nitrogen (N), phosphorus (P), or sulfur (S) to increase surface charge density, improve hydrophilicity, boost antibacterial capabilities, and optimize ion-selective transport [19]. Concurrently, isolating nanocellulose from renewable biomass, such as banana stalks, nipa palm leaves, and sugarcane bagasse, has gained prominence to promote green materials and circular economy frameworks [20]. H. Zhang et al. (2025) highlighted the synergistic resonance between nanocellulose and graphene derivatives in water purification and solar-driven desalination, achieving evaporation efficiencies exceeding 90%[21]. J. Song et al. (2025) developed dual-crosslinked CNF/graphene aerogels capable of simultaneous desalination and per- and polyfluoroalkyl substances (PFAS) removal from seawater [19]. By 2026, Mohammad Usayed Khan and Pabitro Prosad Mondal successfully extracted nanocellulose from banana stalks with a crystallinity index of approximately 66.60%, unlocking the potential of agricultural by-products for advanced filtration membranes [22].

Despite these noteworthy advancements, a distinct research gap persists within the field. The vast majority of international studies rely on commercial nanocellulose or bacterial nanocellulose, whereas the exploitation of local agricultural wastes, such as banana stalks in Vietnam remains underdeveloped. Furthermore, domestic research predominantly focuses on aerogels or adsorbents for wastewater remediation, leaving a scarcity of comprehensive studies on specialized, small-scale desalination membranes intended for domestic water production. In particular, the hybridization of nanocellulose extracted directly from banana stalks with nitrogen/phosphorus co-doped graphene oxide (n-pGO) to simultaneously enhance ion selectivity, mechanical strength, and low-pressure operability has not yet been thoroughly investigated.

Therefore, this study proposes the development of a green nanocomposite membrane based on banana-derived nanocellulose and nitrogen/phosphorus-doped graphene oxide (n-pGO) for desalination applications. In this work, nanocellulose was extracted from banana stalk by-products through sequential alkaline treatment, bleaching, and acid hydrolysis. Simultaneously, nitrogen/phosphorus co-doped graphene oxide (n-pGO) was synthesized via a modified Hummers'

method. The composite Nanocellulose/n-pGO membrane was subsequently fabricated using a layer-by-layer coating method on the nanocellulose substrate to establish highly stable nanochannels for desalination. Additionally, a 1L pilot-scale system was constructed to evaluate the practical applicability of the developed material under realistic conditions.

The obtained nanocomposite membrane exhibited excellent desalination performance with salt rejection exceeding 98% and stable water flux ranging from 160–180 $L \cdot m^{-2} \cdot bar^{-1}$ under atmospheric pressure conditions. The treated water satisfied most requirements of QCVN 01-1:2018/BYT for domestic water quality, including significant reduction of total dissolved solids (TDS), turbidity below 0.2 NTU, and complete removal of E.coli and Coliform bacteria. Additionally, the membrane demonstrated strong antibacterial activity, high antifouling performance with a flux recovery ratio (FRR) above 85% after multiple filtration cycles, and stable surface charge characteristics with a zeta potential of −32.2 mV. These findings indicate the strong potential of banana-derived nanocellulose/n-pGO membranes as low-cost, sustainable, and environmentally friendly desalination materials for saline-affected regions in Vietnam.

2. Methodology

2.1 Materials

Banana pseudostem by-products were collected from banana cultivation farms in Ho Chi Minh City, Vietnam. Following collection, the raw materials were immediately transported to the laboratory at the Biotechnology Center of Ho Chi Minh City. Here, the banana stems were washed thoroughly multiple times with water to eliminate surface dirt and impurities, subsequently sliced into small segments, and dried at 60°C until a constant weight was achieved. The dried banana stems were then finely ground to serve the subsequent cellulose extraction steps.

Regarding the components utilized for membrane coating, Graphene Oxide (GO) was synthesized and modified from pure graphite powder. All chemicals and solvents used in this study, including Sodium Hydroxide (NaOH), Sulfuric Acid (H_2SO_4), Hydrogen Peroxide (H_2O_2), graphite powder, and deionized (DI) water, were supplied by the Biotechnology Center of Ho Chi Minh City. These chemicals were of analytical reagent grade and used directly as received without any further purification processes.

2.2 Extraction of cellulose

After being washed, the banana stem is cut into small pieces about 2-5mm in size and dried at 60–80°C until a constant weight is achieved. Then, the rawmaterials will be treated with NaOH solution (with the concentration of 1 and 2M) at 80–90°C for 2–4h (ratio 1:30). The mixture is filtered, washed to a neutral pH, and dried. Next, the treated fraction is continuing bleached in a composite solution of H_2O_2 (16% w/v) and NaOH (5% w/v) with a volume ratio of 4:1 at 55°C for 90 min, repeating 2–3 times until a uniform white sample is obtaine. Finally, the purified cellulose is hydrolyzed with H_2SO_4 solution (55, 60, and 65 wt%) at 40–45°C for 30–60 min. The post-hydrolysis suspension was repeatedly centrifuged and washed with distilled water, followed by pH adjustment to approximately 6–7. Subsequently, the resulting nanocellulose solution was ultrasonicated for 15 min to disrupt agglomeration and form a stable suspension, which was either

freeze-dried or stored directly in its suspension form.

2.3 Synthesis of Graphene Oxide (GO)

Graphene oxide (GO) was synthesized using a modified Hummers' method [23]. Briefly, graphite powder was dispersed in a mixture of concentrated H_2SO_4 and H_3PO_4 (9:1 v/v) under continuous stirring while maintaining the temperature between 0°C and 5°C. Potassium permanganate ($KMnO_4$) was then slowly added to the suspension. The mixture was stirred continuously for 6h under controlled temperature. After completion of the oxidation reaction, hydrogen peroxide (H_2O_2) was added to terminate the reaction. The resulting mixture was further treated with HCl and deionized (DI) water (1:3 v/v). The obtained GO was separated by centrifugation, thoroughly washed with deionized water until neutral pH, and dried for subsequent use.

2.4 Preparation of possitive graphene oxide

GO was dispersed in deionized water and sonicated for 1h to form a homogeneous suspension. Subsequently, urea was added at a GO-to-urea mass ratio of 1:10 (e.g., 100 mg of GO to 1g of urea), and the mixture was stirred for 60 min. The solution then underwent thermal treatment in a microwave reactor at 120–150°C for 6–12h to facilitate interactions between the urea and the oxygen-containing functional groups on the GO surface. During this process, partial reaction of epoxy and carboxyl groups occurred, leading to the formation of nitrogen-containing moieties (such as amines or amides) alongside a mild reduction of the GO matrix. Post-reaction, the resulting product was washed with deionized water combined with centrifugation (5–8 cycles) to eliminate residual urea, and subsequently dried at 60°C overnight to yield the p-GO material. Compared to pristine GO, the obtained material exhibited distinct surface chemical modifications, characterized by the incorporation of nitrogen-containing functional groups and a shifted surface charge.

2.5 Membrane fabrication

The nanocellulose suspension was ultrasonicated for 10–15 min and cast onto a Petri dish (thickness 1–3 mm). The membrane was dried at 60°C. The composite membrane was then prepared by multi-layer coating of n-pGO onto the nanocellulose substrate using a layer-by-layer assembly technique.

3. Result and Discussion

3.1 Characterization of NanoCellulose

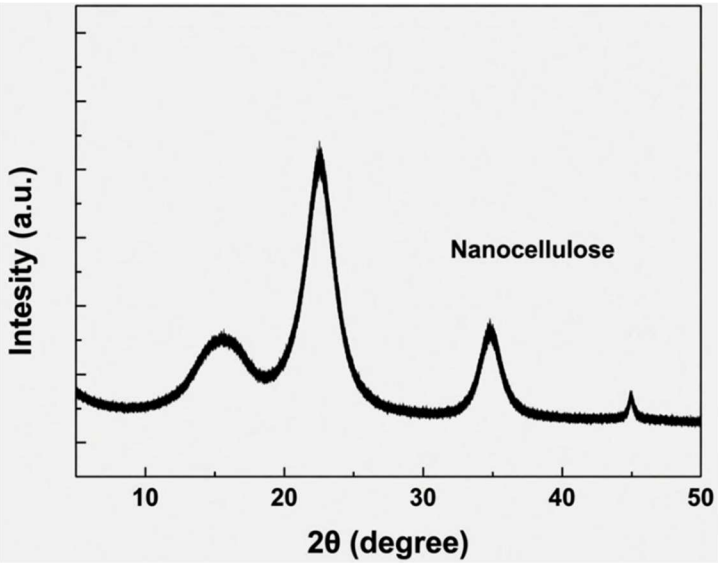

Figure 1. X-ray diffraction (XRD)

Figure 1 illustrates the characteristic diffraction peaks of the Cellulose Iβ structure [24], which represents the predominant crystalline form of cellulose in plant biomass. A sharp and intense diffraction peak emerges at approximately 22.5°, assigned to the (200) lattice plane. The sharpness of this (200) peak indicates that the crystallite size of the nanocellulose lies within the nanoscale. Based on the broadening of this diffraction peak and referencing prior studies on plant biomass-derived cellulose, the crystallite size is estimated to range between 8 and 20 nm.

The intense diffraction signal at $2\theta \approx 22.5°$ is assigned to the (200) plane and represents the most characteristic reflection of Cellulose Iβ [24]. The high intensity and relatively sharp profile of this peak indicate that the extracted nanocellulose possesses a well-preserved crystalline structure and a high degree of molecular ordering. Similar diffraction patterns have been widely reported for nanocellulose isolated from lignocellulosic biomass after chemical purification and acid hydrolysis treatments.

The diffraction peak located at approximately 34.5° corresponds to the (004) crystallographic plane and is associated with the periodic arrangement of cellulose chains along their longitudinal axis. The presence of this peak further confirms the preservation of the native Cellulose Iβ structure and suggests a relatively ordered packing of cellulose nanofibrils. No significant diffraction peaks associated with Cellulose II were observed, indicating that the alkaline and bleaching treatments did not induce substantial polymorphic transformation of the cellulose framework.

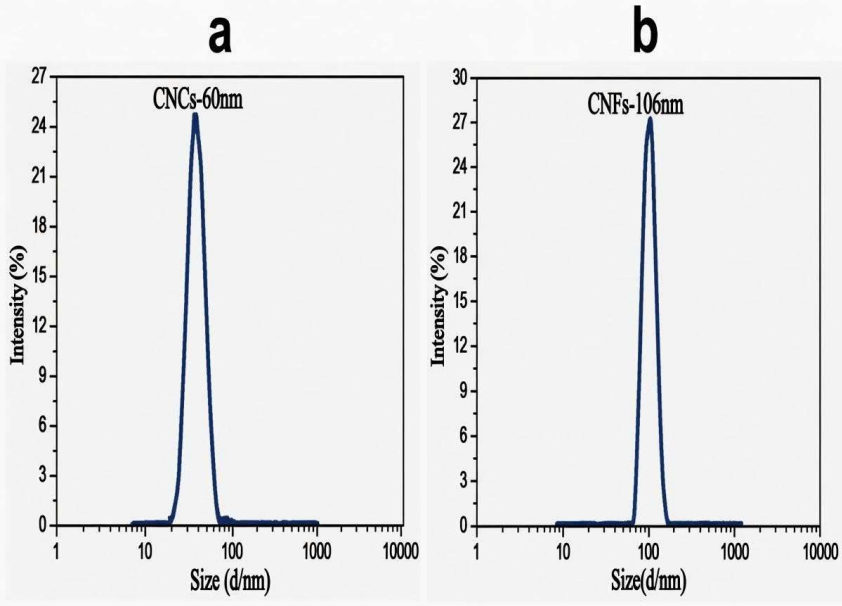

Figure 2. XRD patterns - (a) nanocellulose crystal (CNC) suspension;
(b) nanocellulose fiber (CNF) suspension

Figure 2(a) illustrates that the CNCs sample exhibits a narrow size distribution peak centered primarily around 60 nm, indicating a relatively uniform particle size and excellent dispersibility within the suspension. Conversely, Figure 2(b) shows that the CNFs sample possesses a larger average size distribution of approximately 106 nm, characterized by a broader distribution peak compared to that of the CNCs. Following the nanostructuring process, both CNCs and CNFs successfully maintain the characteristic crystalline structure of pristine cellulose. Nevertheless, CNCs exhibit a higher degree of crystallinity because the amorphous cellulose fractions are more aggressively removed during chemical treatment, whereas CNFs retain a continuous, long fibrillar architecture.

Table 1. Yield of nanocellulose extraction from banana pseudostem

Raw materials	Mass (g)
Crude powder (from banana pseudostem)	30
NanoCellulose	10,47

$$Yield\ (\%) = \frac{m_{NC}}{m_{powder}}\ x\ 100 = \frac{10{,}47}{30}\ x\ 100 = 34{,}9\%$$

The yield of nanocellulose extracted from banana pseudostem was 34.9% (10.47 g of nanocellulose obtained from 30 g of crude banana pseudostem powder), indicating efficient conversion of agricultural waste into high-value nanomaterial.

3.2 Characterization of n-pGO

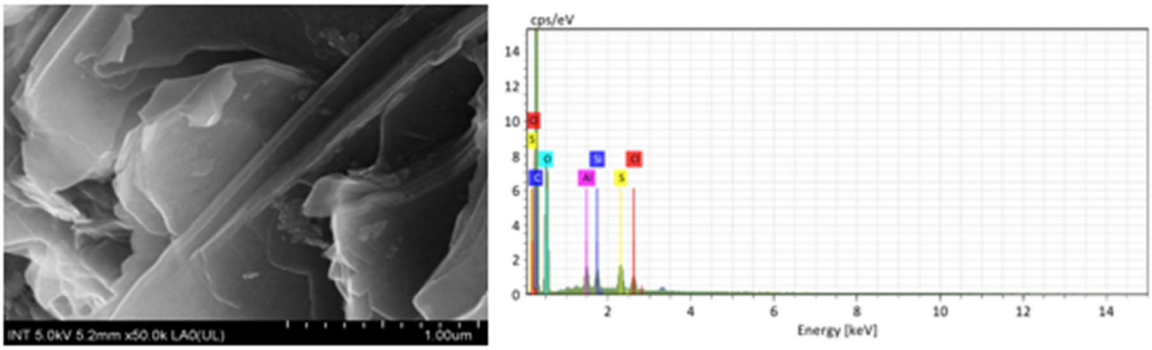

a) b)

Figure 3. SEM micrographs and EDX spectra: (a) SEM image; (b) EDX spectrum.

Figure 3(a) presents the SEM micrograph exhibiting the characteristic layered, sheet-like structure of graphene oxide, which confirms that the graphene layers were successfully oxidized and exfoliated from graphite. The wrinkled surface and layered architecture of GO contribute to an increased specific surface area, thereby facilitating interactions with both nanocellulose and ions within saline solutions. Furthermore, the folds and vacancies between the GO layers serve as structural nanochannels that accelerate water transport and enhance ion selectivity within the composite membrane. Additionally, the porous and irregular structure of GO expands the number of surface active sites, which promotes adsorption capacity and improves the overall hydrophilicity of the material.

Figure 3(b) displays the EDX spectrum featuring prominent characteristic peaks of carbon and oxygen, confirming the presence of oxygen-containing functional groups formed during the oxidation process. Ultimately, these findings are highly consistent with the FTIR and UV-Vis data, thereby validating the synthesis efficiency and chemical structure of the GO prepared via the modified Hummers' method.

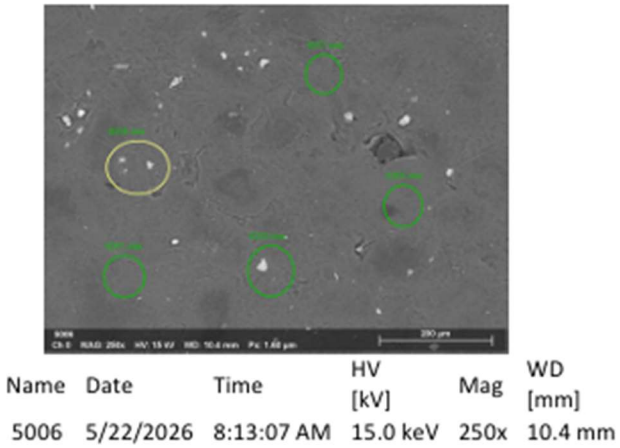

Figure 4. SEM micrographs were acquired at a magnification of 250×; the accelerating voltage was 15 kV

Table 2. Elemental composition

Spectrum	C (%)	N (%)	O (%)	Al (%)	Si (%)	S (%)	Cl (%)	K (%)
8257.xlsx	64.53	–	33.55	0.47	0.37	0.70	0.38	–
8258.xlsx	65.23	–	32.69	0.51	0.42	0.71	0.44	–
8259.xlsx	63.56	–	34.17	0.68	0.22	0.73	0.43	0.20
8260.xlsx	66.64	–	31.77	0.54	–	0.67	0.37	–
8261.xlsx	63.81	1.58	33.00	0.52	–	0.70	0.38	–
Mean	**64.76**	**1.58**	**33.04**	**0.54**	**0.34**	**0.70**	**0.40**	**0.20**
Standard Deviation	**1.24**	**0.00**	**0.90**	**0.08**	**0.11**	**0.02**	**0.03**	**0.00**
Standard Error of the Mean	**0.55**	**0.00**	**0.40**	**0.04**	**0.05**	**0.01**	**0.01**	**0.00**

According to Table 2 and Figure 3(b), the EDX analysis reveals that the synthesized material primarily consists of carbon (64.76 at.%) and oxygen (33.04 at.%), which aligns with the characteristic composition of graphene oxide. The relatively high oxygen content demonstrates that the oxidation of graphite successfully introduced abundant oxygen-containing functional groups onto the material surface. Notably, the detection of nitrogen at a content of 1.58 at.% confirms the successful doping of nitrogen into the graphene oxide framework. Meanwhile, other elements, including Al, Si, S, Cl, and K are present only in trace amounts (<1 at.%), which can be attributed to the chemicals utilized during the synthesis or residual impurities remaining after the washing process. Ultimately, these results confirm that the n-pGO material exhibits a high degree of oxidation and incorporates the essential doped elements required for the fabrication of Nanocellulose/n-pGO desalination membranes.

3.3 Characterization of composite membrane

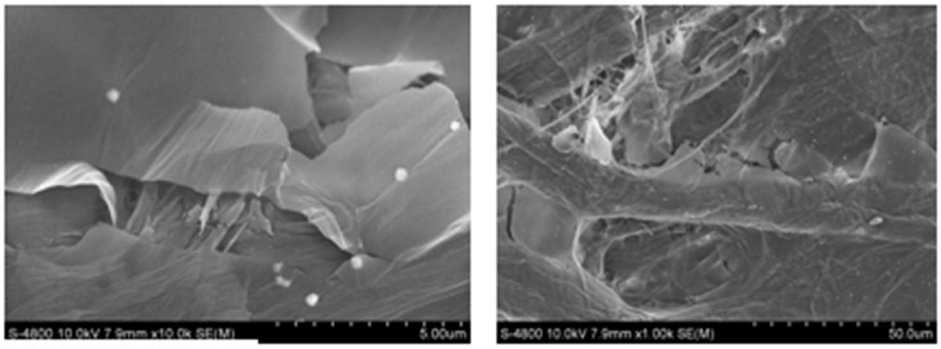

Figure 5. SEM results of the membrane

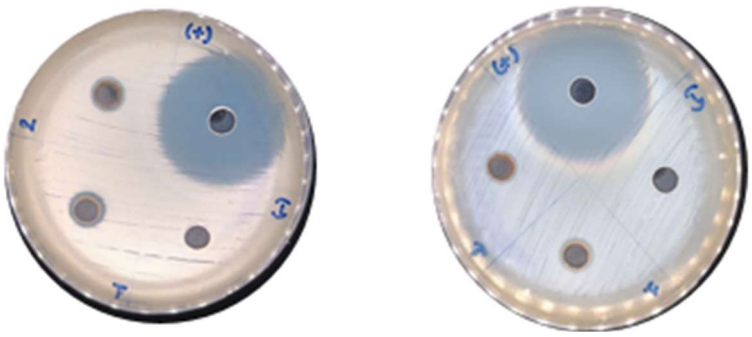

a) b)

Figure 6. Antibacterial activity evaluated by the agar disk diffusion method against: (a) E. coli and (b) Salmonella

The SEM micrographs reveal that the GO-coated biocellulose (BC–GO) membrane possesses a compact and continuous layered morphology. Such a structure is advantageous for membrane filtration because it can provide a more uniform transport pathway while reducing the availability of surface sites for foulant accumulation.

The antibacterial performance of the membranes was evaluated using the agar disk diffusion method. As shown in Figure 6, a distinct inhibition zone was observed around the BC–GO membrane, whereas the pristine BC membrane produced little or no detectable inhibition. These results indicate that the antibacterial activity of the composite membrane is primarily associated with the presence of graphene oxide.

The antibacterial behavior of GO has been widely attributed to several complementary mechanisms. First, the sharp edges of GO nanosheets can interact directly with bacterial cell membranes, causing membrane disruption and leakage of intracellular contents. Second, oxygen-containing functional groups on the GO surface may induce oxidative stress, which can interfere with normal cellular functions and compromise bacterial viability. In addition, the hydrophilic and negatively charged surface of GO can reduce bacterial attachment and hinder the initial stages of biofilm formation.

Further evidence was obtained from SEM observations after bacterial exposure. Compared with the pristine BC membrane, substantially fewer bacterial cells were detected on the surface of the BC–GO membrane. Moreover, some attached cells exhibited distorted or damaged morphologies, suggesting adverse interactions between the bacterial membrane and the GO-coated surface. Although the exact antibacterial mechanism requires further investigation, these observations are consistent with previous reports describing the antimicrobial effects of graphene oxide-based materials.

The results suggest that GO contributes not only to membrane structural stability but also to improved resistance against microbial contamination. This characteristic is particularly beneficial for desalination and domestic water treatment applications, where biofouling is one of the major factors limiting long-term membrane performance.

3.4 Desalination performance

A laboratory-scale filtration system with a treatment capacity of 10 L day^{-1} was constructed to evaluate the performance of the fabricated n-pGO/nanocellulose composite membrane for brackish water treatment. The system was operated in batch mode with a filtration time of 15 min (0.25 h) per cycle at room temperature (25°C).

Prior to membrane filtration, the feed water was pretreated by coagulation using 25 mg L^{-1} polyaluminum chloride (PAC) at pH 7, followed by sedimentation and granular media filtration. The pretreatment unit consisted of two filtration columns with an internal diameter of 0.05 m. Each column was packed with a multilayer filter bed comprising 0.25 m of sand, 0.20 m of activated carbon, and 0.05 m of gravel as a supporting layer.

After pretreatment, the water was directed to the membrane module for desalination. The filtration performance was evaluated using synthetic brackish water containing 4‰ NaCl under atmospheric pressure. All experiments were conducted in triplicate (n = 3) to ensure the reliability and reproducibility of the obtained results.

The head loss through the filter media bed was determined using the Carman–Kozeny equation:

$$h_L = \frac{f}{\varphi}\frac{1-\varepsilon}{\varepsilon^3}\frac{L}{d}\frac{v^2}{g}$$

Where h_L denotes the hydraulic head loss through the porous media layer (m), f is the friction coefficient, φ represents the particle shape factor (sphericity), ε is the porosity of the packed bed, L is the filter bed depth (m), d is the mean particle diameter (m), v is the superficial filtration velocity (m/s), and g is the acceleration due to gravity (9,81 m/s^2).

The total head loss across the filter bed was calculated to be approximately 54 cm of water column, which is acceptable for low-pressure gravity-driven operation. The overall water recovery of the pilot system reached 82% (8.2 L treated water from 10 L feed).

Table 3. Water quality parameters before and after treatment

Parameter	**Unit**	**Raw water**	**BC membrane**	**BC – GO membrane**	**QCVN 01-1:2024/BYT Limit**
Physical	Turbidity	5.2	1.25	0.20NTU	≤ 2 NTU
	Color	35	17		≤ 15 TCU
	Taste and Odor	None	None	None	No objectionable odor or taste
	pH	7.5	7.2	7.2	6.5 – 8.5
Chemical	Amonium (NH_4^+)	0.25	0.21	ND (LOD 0.02 mg/L)	≤ 0.3 mg/L

Parameter	Unit	Raw water	BC membrane	BC – GO membrane	QCVN 01-1:2024/BYT Limit
	Nitrate (NO_3^-)	35	ND (LOD 0.5 mg/L)	ND (LOD 0.5 mg/L)	≤ 50 mg/L
	Iron (Fe)	0.18	ND (LOD 0.01mg/L)	ND (LOD 0.01mg/L)	≤ 0.3 mg/L
	Manganese (Mn)	0.01	ND (LOD 0.005 mg/L)	ND (LOD 0.005 mg/L)	≤ 0.1 mg/L
	Arsenic (As)	0.005	ND (LOD 0.001 mg/L)	ND (LOD 0.001 mg/L)	≤ 0.01 mg/L
	Lead (Pb)	0.004	ND (LOD 0.001 mg/L)	ND (LOD 0.001 mg/L)	≤ 0.01 mg/L
	TDS	320	15	8	≤ 1000 mg/L
Microbiological	E. coli	10^3	ND	ND	0 /100 mL
	Total coliform	10^2	ND	ND	0 /100 mL

The desalination performance of the BC–GO membrane was evaluated using synthetic brackish water with varying NaCl concentrations. The permeation flux (J), salt rejection (R), and flux recovery ratio (FRR) were calculated using the following equations:

$$J = \frac{V}{A.t}$$

$$R(\%) = \frac{C_f - C_p}{C_f} \; x \; 100$$

$$FRR = \frac{J_r}{J_0} x \; 100$$

Where A is the effective membrane area (19.67 cm^2), V is the permeate volume, t is the filtration time, Cp and C_f are the permeate and feed concentrations, and Jr, J_0 are the recovered and initial fluxes, respectively.

The BC–GO membrane exhibited stable fluxes ranging from 160 to 180 $L \cdot m^{-2} \cdot bar^{-1}$ under atmospheric pressure and achieved salt rejection rates above 97–98%. The flux recovery ratio remained higher than 85% after three filtration-cleaning cycles, indicating excellent antifouling properties.

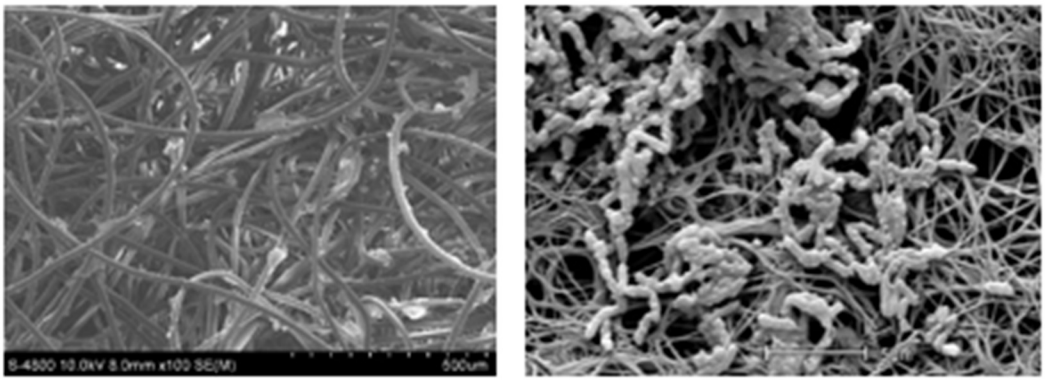

a) b)

Figure 7. SEM micrographs of the membranes post-filtration: (a) BC–GO membrane and (b) BC membrane

The pure BC membrane showed high water permeability but poor salt rejection and severe fouling after operation. In contrast, the BC–GO composite membrane maintained stable flux and high salt rejection (>98%). SEM analysis (Figure 7) revealed significant foulant accumulation and pore blockage on the BC membrane, while the BC–GO surface remained relatively clean.

The enhanced antifouling performance is attributed to the increased hydrophilicity and negative surface charge of the GO layer, which promotes the formation of a hydration layer and generates electrostatic repulsion against foulants.

Overall, the nGO/pGO–nanocellulose composite membrane demonstrated an optimal balance between high water flux, excellent salt rejection, and superior antifouling properties under low-pressure conditions, making it highly promising for small-scale domestic water treatment in salinity-affected areas.

Conclusion

This study successfully developed an n-pGO–nanocellulose composite membrane from banana pseudostem waste. The membrane exhibited high salt rejection, stable water flux under low-pressure conditions, enhanced antibacterial activity, and excellent antifouling performance. Characterization results confirmed the successful integration of n-pGO into the nanocellulose matrix and the preservation of the cellulose structure. The treated water met Vietnamese domestic water quality standards, demonstrating the potential of this membrane for household-scale desalination. Moreover, the use of agricultural waste as a raw material highlights a sustainable and

cost-effective approach for addressing freshwater scarcity in salinity-affected regions of the Mekong Delta.

Acknowledgments

The authors thank the Biotechnology Center of Ho Chi Minh City, Ho Chi Minh City University of Technology (HCMUT) and Vietnam National University (VNU-HCMC) for providing facilities and support for this research.

References

[1] P. Hậu. "Cảnh báo xâm nhập mặn sâu đến 65 km ở ĐBSCL." https://thanhnien.vn/canh-bao-xam-nhap-man-sau-den-65-km-o-dbscl-185230304181027378.htm (accessed 14/3, 2026).

[2] H. Võ, "Xâm nhập mặn năm 2020 dự báo sẽ ở mức độ sâu, gay gắt hơn," ed: VietnamPlus, 2020.

[3] M. Sáng. "Mặn lấn sâu 50 km vào nội đồng Nam Bộ, khuyến cáo khẩn trữ nước ngọt." https://nongnghiepmoitruong.vn/man-lan-sau-50-km-vao-noi-dong-nam-bo-khuyen-cao-khan-tru-nuoc-ngot-d800372.html (accessed 14/3, 2026).

[4] Đ. Hương. "Đợt xâm nhập mặn cao nhất ở Đồng bằng sông Cửu Long dự kiến từ 19–23/3." https://baochinhphu.vn/dot-xam-nhap-man-cao-nhat-o-dong-bang-song-cuu-long-du-kien-tu-19-23-3-102260311121726062.htm?gidzl=_pDvKQt5lqt-Bd5JhD-wJ_mjTLIttxuUuNXo0x6FxntYUdODjDwz4-0h8rYpYBr6j7zsN6HbnVyfgC2-JW (accessed 14/3, 2026).

[5] M. Thắng, "Báo cáo tình hình xâm nhập mặn ĐBSCL," ed: dục và Thời đại, 2024.

[6] Y. Z. Y. W. e. al, "Multilayered graphene oxide membranes for water treatment: A review," vol. 139, pp. 964-981, 2018.

[7] K. S. A. S. S. e. al., "Two-dimensional graphene oxide based membranes for ionic and molecular separation: Current status and challenges," Journal of Environmental Chemical Engineering, vol. 9, no. 4, 2021.

[8] M. D. F. H. J. e. al., "Synthesis of heterogeneous metal organic Framework-Graphene oxide nanocomposite membranes for water treatment," Chemical Engineering Journal, vol. 455, 2023.

[9] S. Yamashita, "Nonlinear optics in carbon nanotube, graphene, and related 2D materials," APL Photonics, vol. 4, 2018.

[10] S. T. H. e. al., "Lightweight and flexible reduced graphene oxide/water-borne polyurethane composites," ACS Appl. Mater. Interfaces, vol. 4, no. 13, pp. 10667-10678, 2014.

[11] M. N. e. al., "Synthesis and applications of carbon nanomaterials for energy generation and storage,'' Beilstein Journal of Nanotechnology," vol. 7, pp. 149-196, 2016.

[12] W. Z. e. al., "Combined Adsorption and Covalent Linking of Paclitaxel on Functionalized Nano-Graphene Oxide," ACS Omega, vol. 3, no. 2, pp. 2396-2405, 2018.

[13] V. e. al., "Layered GO membranes for nanofiltration," 2019.

[14] Z. X. e. al., "One-pot hydrothermal synthesis of Nitrogen-doped graphene," Scientific Reports, vol. 6, 2016.

[15] T. A. e. al., "A Review on the Modification of Cellulose and Its Applications," Polymers, vol. 14, no. 15, 2022.

[16] H. G. e. al., "Incorporation of Cellulose Nanocrystals into Graphene Oxide Membranes for Efficient Antibiotic Removal," ACS Appl. Mater. Interfaces, vol. 13, no. 12, 2021.

[17] A. S. a. S. J. Zaidi, "Progress and Prospects of Nanocellulose-Based Membranes for Desalination and Water Treatment," Membranes, vol. 12, no. 5, p. 462, 2022.

[18] G. D. P. Grzybek, and B. van der Bruggen, "Cellulose-based films and membranes: A comprehensive review," Chemical Engineering Journal, vol. 495, 2024.

[19] J. S. e. al., "Dual-functional nanocellulose/graphene aerogel," 2025.

[20] T. N. e. al., "Nanocellulose and Graphene Oxide Aerogels for Adsorption and Removal Methylene Blue," ACS Omega, vol. 7, no. 1, 2021.

[21] H. Z. e. al., "Nanocellulose–Graphene Derivative Composite Membranes," Membranes, 2025.

[22] M. U. K. a. P. P. Mondal, "Synthesis of nanocellulose from banana plant stem to fabricate PVA based biodegradable nanocomposite films," Next Materials, 2026.

[23] K. F. N. Zaaba, U. Hashim, S. Tan, W. Liu and C. Voon, "Synthesis of Graphene Oxide using Modified Hummers Method: Solvent Influence," Procedia Engineering, vol. 184, pp. 469–477, 2017.

[24] H. C. P. L. Yoshiharu Nishiyama, "Crystal Structure and Hydrogen-Bonding System in Cellulose Iβ from Synchrotron X-ray and Neutron Fiber Diffraction," Journal of the American Chemical Society, vol. 124, no. 31, 2002.